Effective Temperatures of a Driven System Near Jamming

Ian K. Ono,[1] Corey S. O'Hern,[1,2] D. J. Durian,[3] Stephen A. Langer,[4] Andrea J. Liu,[1] and Sidney R. Nagel[2]

[1]*Department of Chemistry and Biochemistry, University of California, Los Angeles, California 90095*
[2]*James Franck Institute, The University of Chicago, Chicago, Illinois 60637*
[3]*Department of Physics and Astronomy, University of California, Los Angeles, California 90095*
[4]*Information Technology Laboratory, NIST, Gaithersburg, Maryland 20899*

(Received 12 October 2001; published 8 August 2002)

Fluctuations in a model of a sheared, zero-temperature foam are studied numerically. Five different quantities that independently reduce to the true temperature in an equilibrium thermal system are calculated. One of the quantities is calculated up to an unknown coefficient. The other four quantities have the same value and all five have the same shear-rate dependence. These results imply that statistical mechanics is useful for the system even though it is far from thermal equilibrium.

DOI: 10.1103/PhysRevLett.89.095703 PACS numbers: 64.70.Pf, 82.70.–y, 83.80.Iz

Statistical mechanics describes the connection between microscopic properties and collective many-body properties in systems in thermal equilibrium. There is no equivalent formalism for driven, athermal systems. Nonetheless, recent phenomenological approaches [1] that assume thermal behavior are surprisingly successful in describing driven glassy materials such as sheared foam. Foam is a dense packing of bubbles in a small amount of liquid, and is athermal because the thermal energy is much smaller than the typical energy barrier for bubbles to change their relative positions [2]. As a result, quiescent foam is *jammed* [2]; it is disordered and has a yield stress. If foam is steadily sheared, it is pushed over energy barriers and flows as different bubble packings are explored. However, it is unclear if this degree of ergodicity is enough to lead to thermal behavior.

In this Letter, we test the assumption that a sheared foam can be modeled as a thermal system with a temperature that depends on shear rate. We conduct numerical simulations of a simple model of sheared foam and measure five quantities that all reduce to the true temperature in a thermal system. Although these quantities must all have the same value in an equilibrium thermal system, there is no guarantee that they should be the same in the steadily sheared model foam. Remarkably, three of the effective temperatures are the same. The fourth can only be calculated up to an unknown constant but has the same shear-rate dependence as the first three, and the fifth cannot be calculated over the same range but matches smoothly to the first three. Our results for the first three effective temperatures are shown as a function of shear rate in Fig. 1 for two different bubble size distributions. In a companion paper, Berthier and Barrat reach similar conclusions for a sheared thermal system [3]. These results suggest that statistical mechanics is indeed useful for describing driven jamming systems.

Our bubble dynamics simulations are carried out in two dimensions on Durian's model of foam [4]. The bubbles are circles with diameters assigned from one of two different distributions. The first (polydisperse) distribution is flat from 0.6 to 1.4 times the average bubble diameter. The second (bidisperse) distribution consists of equal numbers of small and large bubbles of diameter ratio 1.4. We avoid monodisperse systems because they order under shear [5].

Pairs of bubbles only interact, via a repulsive spring, when they overlap; this approximates the energy cost of bubble deformation [4]. There is also a frictional force proportional to the velocity difference between a bubble and the average flow at its position. The system is fully periodic, with flow in the $\hat{x}$ direction and a shear gradient in the $\hat{y}$ direction imposed using the Lees-Edwards boundary condition [6]. We scale lengths by the average diameter d,

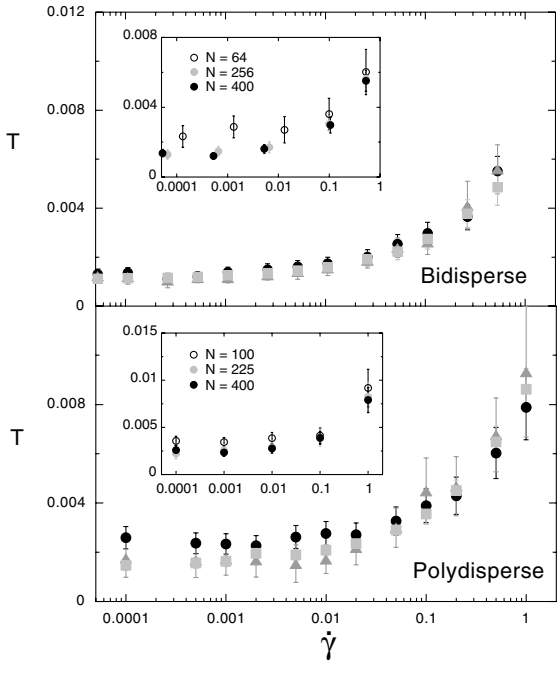

FIG. 1. Four effective temperatures, T_p (circles), T_{xy} (triangles), and T_U (squares), calculated as a function of shear rate. Insets: T_p vs $\dot{\gamma}$ for different system sizes.

energies by kd^2, where k is the spring constant, and time scales by $\tau_0 = b/k$, where b is the friction coefficient. Unless otherwise specified, the systems contain $N = 400$ bubbles at an area fraction of $\phi = 0.9$ (well above random close packing at 0.84). Quantities are measured after initial transients die away and the system has reached steady state. Error bars are based on averages over initial realizations; they are larger in the polydisperse case because the size distribution varies among realizations.

Three of the five calculated effective temperatures are based on linear response relations or fluctuation-dissipation relations. Similar definitions have been used to characterize nonequilibrium systems in the contexts of weak turbulence [7], aging of glassy systems [8], granular packings [9,10], and sheared aging systems [2,11]; such effective temperatures can control the direction of heat flow and thus play the role of temperature in certain nonequilibrium systems with small energy flows [12].

Definition 1: pressure fluctuations.—In an equilibrium system at fixed N, T and area A, the variance of the pressure is given by [6]

$$\langle p\rangle + \frac{\langle x\rangle}{A} - \beta_T^{-1} = \frac{A}{T}\langle(\delta p)^2\rangle, \tag{1}$$

where $\beta_T^{-1} \equiv -A(\partial\langle p\rangle/\partial A)_T$ is the inverse isothermal compressibility, A is the area of the system, p is the pressure, x is the hypervirial [6], and the Boltzmann constant is unity. In our driven, athermal system, we thus define

$$T_p = \frac{A\langle(\delta p)^2\rangle}{\langle p\rangle + \frac{\langle x\rangle}{A} - \beta_T^{-1}}, \tag{2}$$

so that T_p reduces to the true temperature in an equilibrium thermal system. To measure the compressibility, we perturb the system area A and measure the resulting value of $\langle p\rangle$ during shear to calculate the derivative. In simulations of a quiescent system in thermal equilibrium with the same potential and polydispersity, we find that, with comparable statistics, Eq. (2) yields results within 5% of the simulation temperature. Our results for T_p are shown as circles in Fig. 1.

The inset of Fig. 1 shows that T_p is the same for the two larger system sizes studied, $N = 225$ and $N = 400$. At low shear rates, T_p is slightly higher at the smallest size. This is consistent with previous results on velocity correlations, which are independent of N at high shear rates and develop a weak N dependence at low shear rates due to a slower decay of the velocity correlations with distance [13].

Definition 2: shear stress fluctuations.—The viscosity of an equilibrium system is related to the integral over the shear stress autocorrelation function [6]:

$$\eta = \frac{A}{T}\int_0^\infty dt\langle\delta\sigma_{xy}(t)\delta\sigma_{xy}(0)\rangle. \tag{3}$$

We use Eq. (3) to define T_{xy}, calculating the steady-state shear viscosity from $\eta = \langle\sigma_{xy}\rangle/\dot\gamma$. Our results for T_{xy}, shown as triangles in Fig. 1, are in good agreement with T_p at all shear rates. The stress autocorrelation function, used to calculate T_{xy}, is shown for four shear rates in Fig. 2(a). With decreasing $\dot\gamma$, the correlation time increases approximately linearly, while the variance $\langle(\delta\sigma_{xy})^2\rangle$ decreases and then saturates. Note that the correlation function does not decay monotonically at high shear rates. It has been shown that the velocities of neighboring bubbles are anticorrelated at high shear rates, where bubbles collide with each other, but are correlated at low shear rates, when clusters of bubbles rearrange more cooperatively [13].

Definition 3: energy fluctuations.—The constant-area heat capacity of an equilibrium system is related to energy fluctuations:

$$\frac{d\langle U\rangle}{dT} = \frac{\langle(\delta U)^2\rangle}{T^2}. \tag{4}$$

This can be rearranged and integrated on both sides to provide a definition of T_U[9] up to a reference temperature $T_{\rm ref}$. We calculate the absolute magnitude of T_U from the relation between the energy fluctuations, $\langle(\delta U)^2\rangle$, and the average energy, $\langle U\rangle$, shown in Fig. 2(b). We find $\langle(\delta U)^2\rangle = (3.8 \pm 0.2) \times 10^{-3}\langle U\rangle^2$ at high $\langle U\rangle$ (high $\dot\gamma$), which, using Eq. (4), implies $\langle U\rangle = (0.65 \pm 0.05)NT_U$ at high $\dot\gamma$ for both polydisperse and bidisperse systems. We then integrate using Eq. (4) to obtain T_U at all $\dot\gamma$. The high $\dot\gamma$ behavior resembles equipartition except that the coefficient of T_U is not $f/2$, where $f = 2N$ is the number of degrees of freedom. Our potential is a harmonic repulsion with finite range, so equipartition is not exact. The results for T_U, shown as squares in Fig. 1, agree with T_p and T_{xy} at all shear rates for both polydisperse and bidisperse systems.

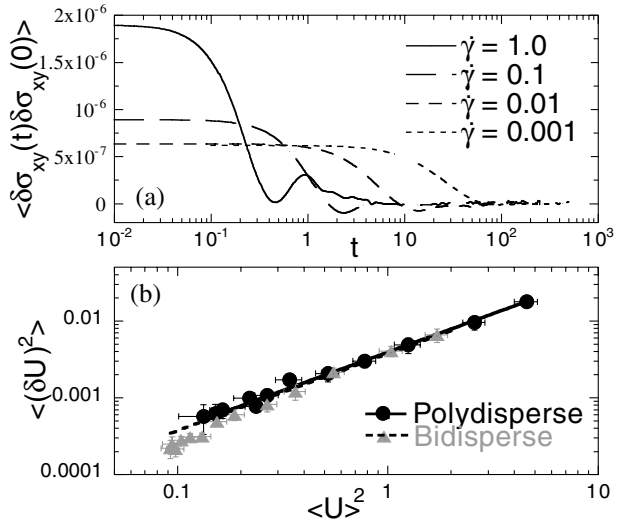

FIG. 2. (a) Shear stress autocorrelation functions at different shear rates for the polydisperse system (see Definition 2). (b) Variance of energy fluctuations plotted against average energy squared (Definition 3). The lines are fits to $\langle(\delta U)^2\rangle \propto \langle U\rangle^2$.

Definition 4: Stokes-Einstein relation.—In equilibrium, the diffusion constant D satisfies

$$D = \frac{T}{C\eta d}, \tag{5}$$

where C is an unknown constant that depends on system size in two dimensions. Thus, Eq. (5) defines a temperature T_D up to a constant. In a sheared thermal system, the diffusion in the x direction (shear direction) is enhanced by the shear (Taylor dispersion [14]) but the diffusion constant in the y direction (shear-gradient direction) is unaffected. Here, we measure diffusion in the y direction, which arises as bubbles jostle each other as they are sheared, with fixed boundary conditions in the y direction [15]. We measure D in the y direction in two different ways and find good agreement: We integrate the velocity autocorrelation function, and we measure the displacement distribution as a function of time from an initial starting position. It is difficult to extract T_D because D and η vary by several orders of magnitude over the range of $\dot{\gamma}$ studied, while their product varies by less than an order of magnitude and has a lot of scatter and large error bars. This definition is therefore most useful as a consistency check: We use T_p from Definition 1 and vary C to obtain the best agreement between the left and the right sides of Eq. (5). Figure 3 shows that the Stokes-Einstein relation is indeed obeyed and verifies that T_D has the same $\dot{\gamma}$ dependence as the others.

Definition 5: Rate of change of entropy with energy.—The fundamental thermodynamic definition of temperature is $1/T = dS/dU$, where S is the entropy. For a foam, we may thus compute another temperature, T_S, by calculating the probability $\Omega(U)$ for a randomly constructed configuration of bubbles at $\phi = 0.9$ to have total potential energy U, and then differentiating $\ln\Omega(U)$ vs U. (The bubbles are massless so there is no kinetic energy.) To calculate the probability distribution $\Omega(U)$, it is straightforward, in principle, to generate configurations at random and tally a histogram of energies. Our results are shown in Fig. 4(a) for bidisperse collections of N bubbles, for several N on a square lattice of $100N$ points (we have verified that the lattice spacing is not large enough to affect T_S). As expected, $\Omega(U)$ is peaked with both low and high energy configurations being rare. Note that, as N increases, the width decreases and the low-U tail steepens. This makes it effectively impossible to accumulate good statistics for low energy configurations, i.e., for those corresponding to the strain rates of the simulations used in Definitions 1–4.

To access the low energy configurations of Fig. 4, we employed the following version of importance sampling. We add bubbles one at a time, but accept trial placements with a probability given by a Boltzmann factor for the energy increase due to the new bubble. If the first $i-1$ bubbles are already fixed and a trial placement of bubble i is rejected, then temporary placements for the remaining $N-i$ bubbles are generated completely at random, and the total energy is computed and binned. Then the $N-i+1$ rejected bubbles are removed and a new trial placement for bubble i is attempted. All the placements of bubble i occurred with equal probability, and the energies of the resulting configurations are thus tallied into the histogram with appropriate weights. When the last bubble N is finally accepted, we have constructed a very unlikely low energy configuration, and have simultaneously sampled a large number of higher energy configurations. Using this trick, we increase our dynamic range in $\Omega(U)$ from only 8 orders of magnitude to over 100. We have verified that the Boltzmann weighting factor does not affect $\Omega(U)$, only the range of U observed.

For a system such as ours that approximately obeys equipartition, one would expect $\log\Omega \propto N\log U$, as shown

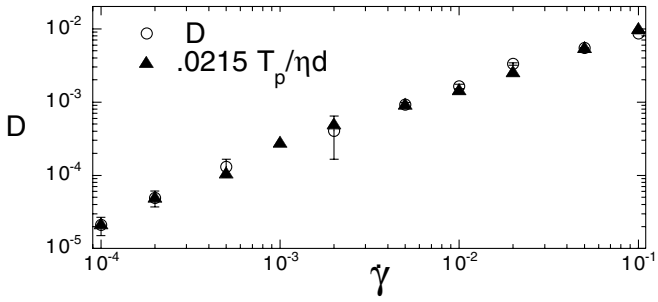

FIG. 3. The Stokes-Einstein relation. The circles represent the diffusion constant D, measured by integrating the velocity autocorrelation function. The triangles represent $T_p/C\eta d$, where C is a constant chosen to obtain the best fit with D.

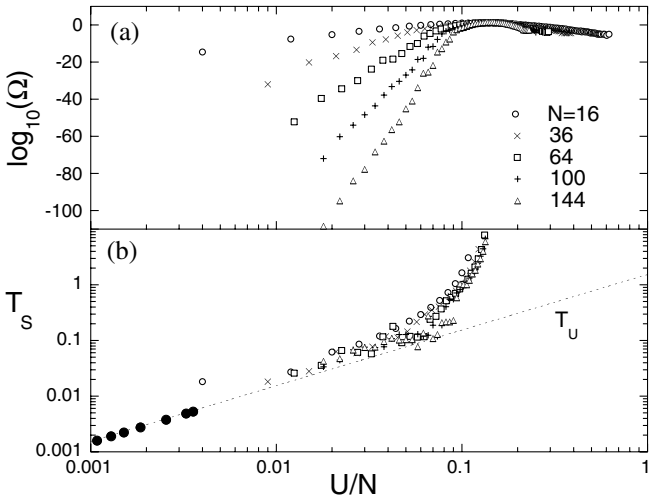

FIG. 4. (a) Probability distribution $\Omega(U)$ of configurations of energy U, for different numbers of bubbles, N for a bidisperse system at $\phi = 0.9$. (b) The temperature T_S (Definition 6) (small symbols). The data from different N collapse on the same curve, and approach the calculated values of T_U (large solid circles) from Definition 3 at small U. The dashed line represents $T_U = U/0.65N$ (see Definition 3).

in Fig. 4(a). The peak in $\log\Omega(U)$ would disappear if kinetic energy were included or if the potential energy were unbounded. Thus, the region above the peak, corresponding to negative temperatures, is unphysical. The very large range of the abscissa makes it appear as if the curves in Fig. 4(a) collapse in the vicinity of the peak, but this is misleading. When $\ln\Omega(U)$ below the peak is differentiated with respect to U to obtain T_S and the result is plotted against U/N, all the data from Fig. 4(a) collapse onto a single curve, as shown in Fig. 4(b).

Although T_S has been calculated over an enormous range of Ω, our measured ranges for T_S and T_U do not overlap. This is shown in Fig. 4(b), where the large solid circles represent T_U from Fig. 1, plotted here as a function of $\langle U\rangle$ instead of $\dot{\gamma}$, while the small symbols represent T_S, calculated from the data in Fig. 4(a). At high $\dot{\gamma}$ (and high $\langle U\rangle$), the bubbles organize into strings parallel to the shear. This is probably a finite-system-size artifact [5], and it affects our results because the system is no longer ergodic [13]. We therefore do not calculate T_U at shear rates above which strings form. Calculations of T_S, on the other hand, are limited to high U because of the statistics shown in Fig. 4(a). Nonetheless, Fig. 4(b) shows that the dependence of T_S on U/N does seem to approach a straight line at sufficiently small U/N, with a slope consistent with the results for T_U. The dashed line is an extrapolation of $T_U = \langle U\rangle/(0.65N)$ beyond the range shown in Fig. 1. The agreement between T_S and T_U is striking because it implies that the sheared system is fully ergodic.

The effective temperatures we have calculated are not easy to measure experimentally. It may be possible to use confocal imaging to extract particle trajectories under shear and to reconstruct the instantaneous stress tensor on each particle, given a known interparticle potential. This would allow calculation of T_p, T_{xy}, T_U, and T_D (Definitions 1–4). Note that T_S (Definition 5) suggests that a thermodynamic interpretation of the effective temperature may be valid. This raises the question of whether the second law of thermodynamics is obeyed and a ''thermometer'' could be constructed—will two systems in thermal contact exchange heat until they reach the same effective temperature [12]? Work is in progress to answer this. At the very least, however, our results show that, given one measurement of effective temperature, one can make predictions based on equality of the others.

Our results raise the need for a criterion for when the concept of effective temperature might be useful. We suggest such a criterion based on the idea underlying the fluctuation-dissipation relation. An analogous concept applies to a steady-state driven system, because the average power supplied to the system must be balanced by the average power dissipated. The power can be dissipated in two ways—by the average flow and by fluctuations around the average flow. We speculate that the concept of effective temperature is useful if nearly all the power supplied by the driving force is dissipated by fluctuations. In the model studied here, all of the power is, by construction, dissipated by fluctuations—the frictional force is proportional to the difference between the velocity of a bubble and the average shear. In systems in the stick-slip regime near jamming, fluctuations typically are large compared to the average flow [2]. This suggests that the concept of effective temperature should be useful for *any* system near the onset of jamming.

We gratefully acknowledge discussions with Jorge Kurchan and Carlos Marques and the support of NSF-DMR-0087349 (A. J. L.), NSF-DMR-0089081 (S. R. N.), and NASA-NAG3-2481 (D. J. D.).

[1] P. Sollich, F. Lequeux, P. Hébraud, and M. E. Cates, Phys. Rev. Lett. **78**, 2020 (1997); P. Hébraud and F. Lequeux, Phys. Rev. Lett. **81**, 2934 (1998); C. Derec, A. Ajdari, and F. Lequeux, Eur. Phys. J. E **4**, 355 (2001).

[2] See *Jamming and Rheology*, edited by A. J. Liu and S. R. Nagel (Taylor & Francis, New York, 2001), and references therein.

[3] L. Berthier and J.-L. Barrat, preceding Letter, Phys. Rev. Lett. **89**, 095702 (2002).

[4] D. J. Durian, Phys. Rev. Lett. **75**, 4780 (1995); Phys. Rev. E **55**, 1739 (1997).

[5] S. Butler and P. Harrowell, J. Chem. Phys. **105**, 605 (1996).

[6] M. P. Allen and D. J. Tildesley, *Computer Simulation of Liquids* (Oxford University Press, New York, 1987).

[7] P. C. Hohenberg and B. I. Shraiman, Physica (Amsterdam) **37D**, 109 (1989).

[8] L. F. Cugliandolo and J. Kurchan, Phys. Rev. Lett. **71**, 173 (1993).

[9] E. R. Nowak, J. B. Knight, E. Ben-Naim, H. M. Jaeger, and S. R. Nagel, Phys. Rev. E **57**, 1971 (1998).

[10] H. Makse and J. Kurchan, Nature (London) **415**, 614 (2002).

[11] J.-L. Barrat and L. Berthier, Phys. Rev. E **63**, 012503 (2001).

[12] L. F. Cugliandolo, J. Kurchan, and L. Peliti, Phys. Rev. E **55**, 3898 (1997).

[13] I. K. Ono, S. Tewari, S. A. Langer, and A. J. Liu (unpublished).

[14] G. I. Taylor, Proc. R. Soc. London A **219**, 186 (1954); **223**, 446 (1954).

[15] S. A. Langer and A. J. Liu, Europhys. Lett. **49**, 68 (2000).